Initial surface reactions in atomic layer deposition of Al_2O_3 on the hydroxylated GaAs(001)-4 × 2 surface

2005 J. Phys.: Condens. Matter 17 7517

(http://iopscience.iop.org/0953-8984/17/48/005)

INSTITUTE OF PHYSICS PUBLISHING JOURNAL OF PHYSICS: CONDENSED MATTER

J. Phys.: Condens. Matter **17** (2005) 7517–7522 doi:10.1088/0953-8984/17/48/005

Initial surface reactions in atomic layer deposition of Al_2O_3 on the hydroxylated GaAs(001)-4 × 2 surface

Hong-Liang Lu, Wei Chen, Shi-Jin Ding, Min Xu, David Wei Zhang[1] and Li-Kang Wang

State Key Laboratory of ASIC and System, Department of Microelectronics, Fudan University, Shanghai 200433, People's Republic of China

E-mail: dwzhang@fudan.edu.cn and dwzhang@fudan.ac.cn

Received 25 August 2005
Published 11 November 2005
Online at stacks.iop.org/JPhysCM/17/7517

Abstract

Hybrid density functional theory has been used to investigate the initial surface reaction mechanism in atomic layer deposition (ALD) of Al_2O_3 on the hydroxylated GaAs(001)-4 × 2 surface. The precursors for ALD of Al_2O_3 are trimethylaluminium (TMA) and H_2O as the aluminium and oxygen sources. For the first half-reaction between TMA with the GaAs surface the calculated activation barrier is 15.4 kcal mol^{-1}, and the H_2O half-reaction proceeds by a mechanism similar to that of the first half-reaction, resulting in an activation barrier of 27.6 kcal mol^{-1}. Both half-reactions are thermodynamically favourable, exothermic by 52.0 and 43.6 kcal mol^{-1} relative to the reactants, respectively.

(Some figures in this article are in colour only in the electronic version)

1. Introduction

GaAs-based metal–oxide–semiconductor field-effect transistors (MOSFETs) have been investigated intensively in the past three decades, driven by their applications in a high-speed circuit, with a low leakage current and high breakdown fields [1–6]. The inherent advantages of GaAs semiconductor include high carrier mobility, large energy band gap and low power consumption [7, 8]. However, most of the current commercialized GaAs-based electronic devices employ Schottky junctions for the gate because of the lack of a suitable gate insulator. Unlike the electrically passive Si–SiO_2 system, the thermal oxidation of the compound semiconductors induces complicated oxidation states at the interface and results in poor electrical properties. High-quality insulators are then desirable for their very low leakage current, and large charge control of both holes and electrons. The deposition of dielectrics on

[1] Author to whom any correspondence should be addressed.

the GaAs substrates by various deposition methods has been shown to reduce the interface-state density and is therefore being studied widely [9–12].

Of the proposed alternative gate dielectrics for the MOSFET, aluminium oxide (Al_2O_3) is considered to be one of the probable candidates for the gate dielectric because of its high dielectric constant, wide bandgap and good thermal stability [13–15]. Atomic layer deposition (ALD) is expected to be a promising technique for growing ultrathin Al_2O_3 films. This technique utilizes alternate pulsing of the precursor gases and vapours onto the solid substrate surface and subsequent chemisorportion or surface reaction of the precursors. The reactant is purged with an inert gas between the precursor pulses. The self-limiting nature of ALD facilitates the growth of uniform thin films with accurate thickness over large areas.

There have been many studies on ALD of Al_2O_3 thin films on the Si-based surface using trimethylaluminium ($Al(CH_3)_3$) and H_2O as precursors, both experimentally as well as theoretically [16–22]. Recently the process of Al_2O_3 growth on the GaAs substrate by ALD has been investigated, too [8, 23–26]. Therefore it is also essential to detailed understand the reaction mechanism of Al_2O_3 ALD on the GaAs-based surface theoretically. In the present work, first-principles calculations based on hybrid density functional theory (DFT) are carried out to investigate the initial surface reactions of Al_2O_3 ALD on the hydroxylated GaAs(001)-4 × 2 surface using $Al(CH_3)_3$ (TMA) and H_2O as precursors to explore the film growth mechanism. This work focuses on analyses of the reaction pathways and changes of the representative bond lengths for these reactions in the gas phase.

2. Calculation method

The initial surface reactions of Al_2O_3 ALD between the precursors, TMA and H_2O, and the hydroxylated GaAs(001)-4 × 2 surface can be separated into two half-reactions

$$GaAs\text{–}OH^* + Al(CH_3)_3 \rightarrow GaAs\text{–}O\text{–}Al(CH_3)_2^* + CH_4 \quad (R1)$$

$$GaAs\text{–}O\text{–}Al(CH_3)_2^* + H_2O \rightarrow GaAs\text{–}O\text{–}Al(CH_3)OH^* + CH_4 \quad (R2)$$

where the asterisks denote the active surface species. The first half-reaction (R1) involves the reaction between the gaseous TMA and a surface hydroxyl group bonded directly to the underlying GaAs substrate. (R2) represents the second half-reaction in which H_2O reacts with a surface Al–CH_3 group, regenerating the surface –OH group. The two half-reactions are separated by an inert gas (e.g., N_2) purging period. The hydroxylated GaAs(001)-4 × 2 surface is simulated using a $Ga_4As_5O_3H_{13}$ cluster, as shown in figure 1. The 'bulk' arsenic and gallium atoms are terminated by hydrogen atoms to avoid spin and charge contamination from the truncated dangling bonds. The number of H atoms is chosen so that the number of nonbonding electrons equals twice the number of threefold coordinated As atoms [27, 28]. The structure has been clearly proposed by Huang *et al*, who used ammonia solution to etch the GaAs wafer, enriching OH radical formation on its surface [29, 30].

The surface half-reactions are investigated using the DFT method with the B3–LYP hybrid density functional, which corresponds to Becke's three-parameter exchange functional (B3) along with the Lee–Yang–Parr gradient-corrected correlation functional (LYP) [31]. The electronic wavefunction is expanded in a Gaussian basis set. All of the atoms are described using the 6-31G(d) basis set. The reaction path from reactants to products is constructed by connecting the transition states with the intermediates. The optimizations are performed without any geometric constraints or symmetry restrictions. Frequency calculations are carried out after geometry optimizations to verify whether a minimum or a first-order saddle point is reached and energies reported here include zero-point energy corrections. All energy

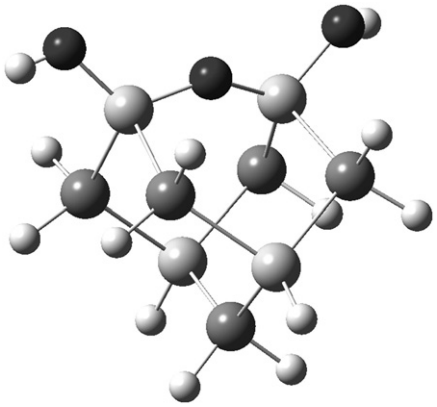

Figure 1. Structure of the $Ga_4As_5O_3H_{13}$ cluster representing the GaAs–OH* surface. The black, light grey, dark grey, and white atoms represent O, Ga, As, and H atoms, respectively.

minimum structures are confirmed to have zero imaginary frequencies, while the transition state structures are further confirmed by only one imaginary frequency. All of the quantum chemical calculations of structures and energies presented in this work are carried out with the aid of the Gaussian 03 set of programs [32].

3. Results and discussion

The reaction pathway for the first half-reaction (R1) is shown in figure 2. The lengths of representative bonds shown with dashed lines in figure 2 and the corresponding reaction energies at 0 K are listed in table 1. As TMA approaches the GaAs–OH* surface, it forms a TMA chemisorbed state (TMA-CS) through the interaction between an empty p-orbital of the Al atom and the oxygen lone-pair electrons from the surface –OH. The electron donation from an oxygen lone pair to the Al atom weakens the Al–C bonds. The Al–C bond length increases from 1.97 Å in TMA to 2.0 Å in the TMA-CS. As shown in figure 2 and table 1, the adsorption energy is calculated to be 31.5 kcal mol^{-1}. Subsequently, TMA-CS transfers the H atom from the hydroxyl group to the methyl ligand by undergoing a transition state (TMA-TS) with an activation barrier of 15.4 kcal mol^{-1} relative to the TMA-CS. At last, the surface changes its functional groups from a GaAs–OH* to GaAs–O–$Al(CH_3)_2^*$ surface after the CH_4 desorption state (CH_4-DS1) is reached. The by-product CH_4 is not bound to the surface in this reaction and can desorb from the surface spontaneously. It is obvious that the overall reaction is exothermic by 52.0 kcal mol^{-1} relative to the reactants, suggesting that the first half-reaction is thermodynamically favourable. The TMA-TS structure has Al–C and O–H bond lengths of 2.21 and 1.19 Å, which are elongated by 10% and 24% with respect to the TMA-CS. During the process of TMA-CS → TMA-TS, the O–Al bond and the H–C bond change from 1.98 and 2.88 Å to 1.88 and 1.50 Å, respectively. All of them indicate the formation of the Al–O bond and the by-product CH_4.

After the initial TMA exposure and following a purge period, the second half-reaction (R2) proceeds through the reaction between water and Al–CH_3 groups. The corresponding reaction pathway is shown in figure 3. In addition, the lengths of representative bonds shown with dashed lines in figure 3 and the corresponding reaction energies at 0 K for this half reaction are also summarized in table 2. The first step of this half reaction involves the adsorption of H_2O onto the GaAs–O–$Al(CH_3)_2^*$ surface to form a H_2O chemisorbed state (H_2O-CS). Our calculation results show that the adsorption energy is also 31.5 kcal mol^{-1}. This stable H_2O-CS is formed where the interaction between an empty p orbital of the Al atom and the oxide

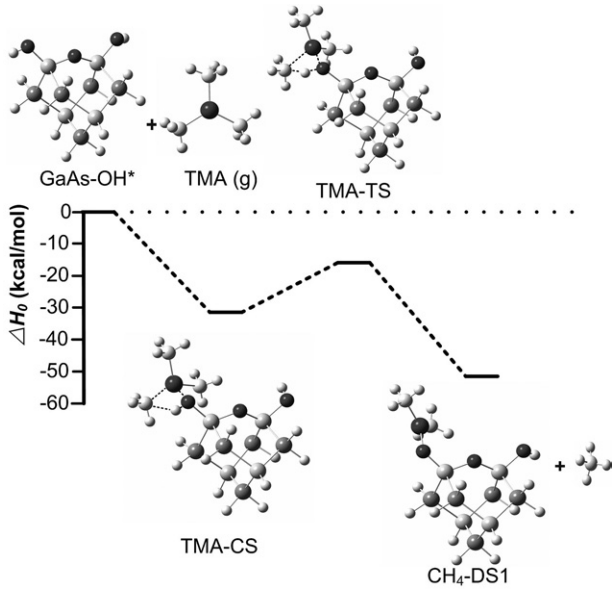

Figure 2. Reaction pathway and optimized geometries for the reaction of gaseous TMA on the GaAs–OH* surface. TMA-CS, TMA-TS, and CH_4-DS1 represent the TMA chemisorbed state, transition state, and CH_4 desorption state, respectively. The representative bonds are shown with dashed lines. The black, light grey, dark grey, small white, white, and large black atoms represent O, Ga, As, H, C, and Al atoms, respectively.

Table 1. Representative bond lengths for the structures of TMA-CS and TMA-TS and reaction energies at 0 K (ΔH_0) for the GaAs–OH*+ TMA half-reaction. All bond lengths are shown in Å while energies are shown in kcal mol^{-1}.

	O–Al	O–H	Al–C	H–C	ΔH_0
TMA-CS	1.98	0.97	2.00	2.88	−31.5
TMA-TS	1.88	1.19	2.21	1.50	−16.1
CH_4-DS1	—	—	—	—	−52.0

lone-pair electrons occurs. The weakened Al–C bond increases from 1.97 Å in the GaAs–O–Al$(CH_3)_2^*$ to 1.98 Å in the H_2O-CS. Then the hydrogen atom from H_2O abstracts a surface methyl group, and reaches the CH_4 desorption state (CH_4-DS2) to complete the half-reaction. Finally, it regenerates the surface –OH groups and again evolves CH_4. The transition state (H_2O-TS) for this half-reaction is found to be 3.9 kcal mol^{-1} lower in energy than the reactants. Therefore, the activation barrier for (R2) is calculated to be 27.6 kcal mol^{-1}. The Al–C and O–H bond distances over the course of the reaction show values of 1.98 and 0.97 Å in the H_2O-CS, elongating to 2.16 and 1.20 Å in the H_2O-TS, respectively. Finally, the CH_4 desorption state (CH_4-DS2) is reached to complete the half-reaction. The overall reaction is exothermic by 43.6 kcal mol^{-1} relative to the reactants, suggesting that the second half-reaction is also energetically favourable.

As can be seen from figures 2 and 3, both half-reactions proceed with a similar reaction mechanism, through separated reactants, the chemisorbed state, transition state, and desorption state. By comparison of the reaction pathways between (R1) and (R2), we can see that the activation barrier and product free energy for (R1) are all lower than those for (R2). As a result,

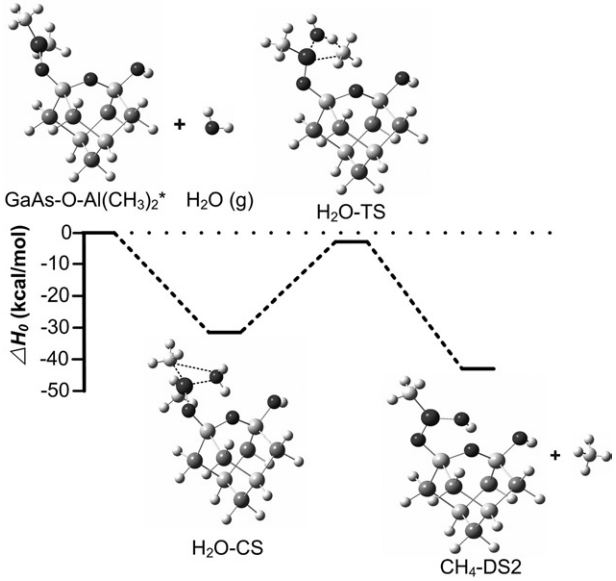

Figure 3. Reaction pathway and optimized geometries for the reaction of H_2O on the GaAs–O–Al$(CH_3)_2^*$ surface. H_2O-CS, H_2O-TS, and CH_4-DS2 represent the H_2O chemisorbed state, transition state, and CH_4 desorption state, respectively. The representative bonds are shown with dashed lines. The black, brown, light grey, dark grey, small white, and large black atoms represent O, Ga, As, H, C, and Al atoms, respectively.

Table 2. Representative bond lengths for the structures of H_2O-CS and H_2O-TS and reaction energies at 0 K (ΔH_0) for the GaAs–O–Al$(CH_3)_2^*$ + H_2O half reaction. All bond lengths are shown in Å while energies are shown in kcal mol^{-1}.

	O–Al	O–H	Al–C	H–C	ΔH_0
H_2O-CS	1.99	0.97	1.98	3.22	−31.5
H_2O-TS	1.90	1.20	2.16	1.50	−3.9
CH_4-DS2	—	—	—	—	−43.6

a little longer H_2O pulse probably is favourable for the reaction product formation. This case is similar to ALD of Al_2O_3 on the hydroxylated Si, Al_2O_3 and SAM surfaces [20–22]. The corresponding experimental result has also been reported by Matero *et al* [17].

4. Conclusions

In summary, the initial reaction mechanism of Al_2O_3 atomic layer deposition using TMA and H_2O as precursors on the hydroxylated GaAs(001)-4 × 2 surface has been investigated using density functional theory calculations. The reaction pathways of both TMA and H_2O half-reactions are presented. The stable chemisorbed intermediates have the same surface adsorption energies of 31.5 eV. The activation barriers for (R1) and (R2) are calculated to be 15.4 and 27.6 kcal mol^{-1}, respectively. The calculation results show that both half-reactions are thermodynamically and kinetically favoured, exothermic by 52.0 and 43.6 kcal mol^{-1} relative to the reactants, respectively. However, a little longer H_2O pulse probably favours the reaction products because the activation barrier and product free energy for (R1) are all lower than those for (R2). The representative bond lengths of both half-reactions are also presented.

Acknowledgments

The work is supported by the National Natural Science Foundation of China, the Science and Technology Committee of Shanghai under grant No 04JC14013, and the Programme for New Century Excellent Talents in University (NCET).

References

[1] Hong M, Kwo J, Kortan A R, Mannaerts J P and Sergent A M 1999 *Science* **283** 1897
[2] Mimura T and Fukuta M 1980 *IEEE Trans. Electron Devices* **27** 1147
[3] Chen E L, Holonyak N and Maranowski S A 1995 *Appl. Phys. Lett.* **66** 2688
[4] Jun B K, Kim D H, Leem J Y, Lee J H and Lee Y H 2000 *Thin Solid Films* **360** 229
[5] Liyama K, Kita Y, Ohta Y, Nasuno M, Takamiya S, Higashimine K and Ohtsuka N 2002 *IEEE Trans. Electron Devices* **49** 1856
[6] Yang J K, Kang M G and Park H H 2004 *J. Appl. Phys.* **96** 4811
[7] Passlack M, Hong M, Mannaerts J P, Opila R L, Chu S N G, Moriya N, Ren F and Kwo J R 1997 *IEEE Trans. Electron Devices* **44** 214
[8] Ye P D, Wilk G D, Kwo J, Yang B, Gossmann H-J L, Frei M, Chu S N G, Mannaerts J P, Sergent M, Hong M, Ng K K and Bude J 2003 *IEEE Trans. Electron Devices* **24** 209
[9] Houng M P, Wang Y H, Huang C J, Huang S P and Horng J-H 2000 *Solid State Electron.* **44** 1917
[10] Lefebvre P R, Lai L and Irene E A 1998 *J. Vac. Sci. Technol.* B **16** 996
[11] Kim T W and You Y S 2001 *Mater. Res. Bull.* **36** 747
[12] Hong M, Ren F, Kuo J M, Hobson W S, Kwo J, Mannaerts J P, Lothian J R and Chen Y K 1998 *J. Vac. Sci. Technol.* B **16** 1398
[13] Wilk G D, Wallace R M and Anthony J M 2001 *J. Appl. Phys.* **89** 5243
[14] Robertson J 2004 *Eur. Phys. J. Appl. Phys.* **28** 265
[15] Gusev E P, Cartier E, Buchanan D A, Gribelyuk M, Copel M, Okorn-Schmidt H and D'Emic C 2001 *Microelectron. Eng.* **59** 341
[16] Puurunen R L 2005 *J. Appl. Phys.* **97** 121301
[17] Matero R, Rahtu A, Ritala M, Leskela M and Sajavaara T 2000 *Thin Solid Films* **368** 1
[18] Frank M M, Chabal Y J, Green M L, Delabie A, Brijs B, Wilk G D, Ho M-Y, da Rosa E B O, Baumvol I J R and Stedile F C 2003 *Appl. Phys. Lett.* **83** 740
[19] Kuse R, Kundu M, Yasuda T, Miyata N and Toriumi A 2003 *J. Appl. Phys.* **94** 6411
[20] Halls M D and Raghavachari K 2004 *J. Phys. Chem.* B **108** 4058
[21] Widjaja Y and Musgrave C B 2002 *Appl. Phys. Lett.* **80** 3304
[22] Xu Y and Musgrave C B 2004 *Chem. Mater.* **16** 646
[23] Ye P D, Wilk G D, Yang B, Kwo J, Chu S N G, Nakahara S, Gossmann H-J L, Mannaerts J P, Hong M, Ng K K and Bude 2003 *Appl. Phys. Lett.* **83** 180
[24] Frank M M, Wilk G D, Starodub D, Gustafsson T, Garfunkel E, Chabel Y J, Grazul J and Muller D A 2005 *Appl. Phys. Lett.* **86** 152904
[25] Ye P D, Wilk G D, Yang B, Chu S N G, Ng K K and Bude J 2005 *Solid State Electron.* **49** 790
[26] Ye P D, Wilk G D, Tois E E and Wang J J 2005 *Appl. Phys. Lett.* **87** 13501
[27] Fu Q, Li L, Li C H, Begarney M J, Law D C and Hicks R F 2000 *J. Phys. Chem.* B **104** 5595
[28] Fu Q, Li L and Hicks R F 2000 *Phys. Rev.* B **61** 11034
[29] Huang C J, Houng M P, Wang Y H and Wang H H 1999 *J. Appl. Phys.* **86** 7151
[30] Houng M P, Huang C J, Wang Y H, Wang N F and Chang W J 1997 *J. Appl. Phys.* **82** 5788
[31] Becke A D 1993 *J. Chem. Phys.* **98** 1372
[32] Frisch M J *et al* 2003 *Gaussian 03, Revision B. 05* (Pittsburgh, PA: Gaussian)